Reshaping Periodic Light Pulses Using Cascaded Uniform Fiber Bragg Gratings

Naum K. Berger, Boris Levit, and Baruch Fischer

***Abstract*—The authors demonstrate the use of cascaded uniform fiber Bragg gratings (FBGs) for the generation of periodic optical pulses with arbitrary waveform. It is a significantly simplified structure compared to complex FBG shapes. The pulse shaping is based on splitting of the input pulses by low-reflecting FBGs into a number of replicas and their superposition with proper amplitude, time delay, and phase shift that depend on the FBG parameters. The reflection amplitude and phase of each grating are unambiguously determined by the needed pulse shape. This method was experimentally verified for converting sinusoidally phase-modulated radiation of continuous-wave laser diode into a Gaussian pulse train with a pulsewidth of 30 ps. A method for controlling the parameters of FBGs during their fabrication process is also presented. It is done by measuring the spectral interference between the reflections from the FBGs and the fiber end by an optical spectrum analyzer and performing a fast Fourier transform. The method allows correction of the FBGs until the needed parameters are obtained during the writing process, as well as at any time after that.**

***Index Terms*—Arbitrary waveform, FBG control, fiber Bragg gratings (FBGs), optical-pulse shaping.**

I. Introduction

THE DEVELOPMENT of all-optical techniques for the manipulation and reshaping of optical pulses has a great importance for ultrahigh-capacity optical communication, nonlinear fiber optics, coherent or quantum control, and for other applications [1]. Conventional methods for pulse shaping are mostly based on time-to-space conversion in bulk [1] or arrayed-waveguide gratings [2]. In such devices, the incident pulse is first spatially (and accordingly spectrally) dispersed by a first diffractive grating and lens along a spatial modulator, then, it is filtered and recombined by a second lens and a diffractive grating, which compensates the induced dispersion. As a spectral filter, one can use a fixed mask [3], programmable liquid crystal [4], or acousto-optic [5] spatial modulators. The use of a programmable spatial modulator allows realizing adaptive real-time pulse shaping [6], in which a desired pulse shape can be achieved without previous characterization of the pulse to be reshaped. The spectral filtering of the input pulse was also performed in the time domain [7]. In this case, the pulse was temporally (and spectrally) dispersed and compressed by a fiber-grating system, and a temporal electrooptic modulator between the two dispersions was used instead of a spatial modulator.

Manuscript received September 18, 2005; revised April 3, 2006.

The authors are with the Department of Electrical Engineering, Technion—Israel Institute of Technology, 32000 Haifa, Israel.

Digital Object Identifier 10.1109/JLT.2006.875944

Recently, fiber Bragg gratings (FBGs) were shown to provide an in-fiber pulse shaper [8]–[12]. The advantages of FBGs are in their simplicity, compactness, and inherent ability to be integrated in all-fiber systems, needed, for instance, in optical communication. The pulse shaper consisting of two step-chirped FBGs with the opposite dispersion signs [8] is similar in its idea to the aforementioned bulk zero dispersion system [1]. The difference is only in the lack of the mask between the two dispersion parts. The needed spectral phase shift is encoded in the spatial structure of the second chirped grating, and it also can function as a spectral phase-only filter. An analogous use of a single chirped FBG for pulse shaping was demonstrated in [9] and [10]. Grating apodization was made to have a form that fits the spectrum of the shaped pulse, and uncompensated grating chirp was used for additional pulse-rate multiplication [9] or for achieving the condition for spectrum-time conversion [10], in which the shape of the output pulse resembles its spectrum. Grating chirp is not so necessary for pulse shaping by an FBG. Rectangular picosecond pulses were obtained with a superstructured FBG [11] without any chirp. For a weakly reflecting grating, the spatial refractive index modulation profile of the grating is given by the Fourier transform of the needed spectral response of the shaping FBG.

Generally, an apodized (superstructured) FBG for pulse shaping can be considered as a spectral filter with a transfer function converting the spectrum of the input pulse to that of the target pulse [11]. Such filter is equally suitable both to a single pulse and to a pulse train with an identical pulse shape. However, for the shaping periodical pulses, the transfer function ought to be determined only for a discrete number of frequencies, corresponding to the spectral harmonics of the input-pulse train. The values of the transfer function can be arbitrary for the other frequencies. This situation substantially simplifies the needed structure of an FBG shaper. It was shown in [12] that the conversion from bright-to-dark periodic soliton pulses can be performed with a single uniform FBG with properly chosen grating parameters. However, it could provide only an approximate solution, and just for this particular case. As was pointed out in that paper [12], the number of free parameters was insufficient for obtaining the exact pulse shape.

In this paper, we demonstrate that the arbitrary shape (amplitude and phase) of periodic optical pulses can be obtained by using a number of consecutive equidistant uniform FBGs with reflectivity and reflection phase of each grating determined by the needed pulse shape. For weak reflection, each grating produces a weighted, phase shifted, and time delayed replica of the input pulse. All of these replicas are superimposed, and their superposition and interference give the pulse with the

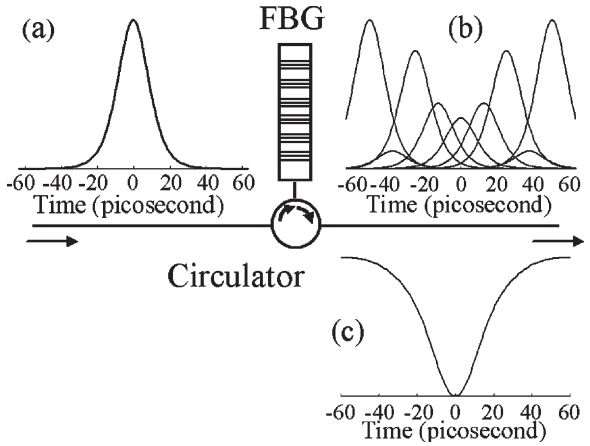

Fig. 1. Pulse shaping by uniform FBGs: conversion of bright-to-dark soliton pulses.

desirable shape. We describe a method for FBG control during the writing process for obtaining the gratings with the required reflectivity and reflection phase. The method allows correcting the reflection phase not only at the time of the grating production, but also at any time after that. For the demonstration of the pulse reshaping, we chose as, an example, the conversion of sinusoidal phase modulated continuous-wave (CW) light into a Gaussian pulse train. We performed the simulations and experiments with CW laser diode and a shaper consisting of six uniform gratings, and obtained good agreement. The advantage of the pulse shaping with uniform FBGs is its simplicity and also its possibility to correct the shaper if changes occur.

II. Method for the Pulse Reshaping

The principle of the pulse shaping with uniform FBGs is demonstrated in Fig. 1. The input pulse to be reshaped [Fig. 1(a)] is reflected from M equidistant uniform FBGs. The distance between the gratings is chosen to provide the time delay T/M between the adjacent replicas, where T is the pulse train period. We assume that the reflection of each grating is low so that multiple reflections can be neglected. Thus, the input pulse reflecting from the gratings is split into M replicas, each with its amplitude, time delay, and phase shift defined by the reflectivity and the reflection phase of each grating. The reflected pulse replicas overlap and interfere in the time domain. It is shown below that by proper choice of the grating reflectivities and reflection phases, the desired pulse shape can be obtained as a result of this interference. Such reshaping is shown in Fig. 1, where the conversion from bright-to dark soliton pulses by ten uniform FBGs is demonstrated. The input periodic pulses (Fig. 1(a) shows only one period) are split into ten time-delayed replicas [Fig. 1(b)]. Superposition of the pulse replicas gives the dark soliton pulse shown in Fig. 1(c).

Mathematically, the problem is formulated in the following form. For reshaping of the input-pulse train, we have to know its complex field spectrum $F_{\rm in}(\omega)$, the field spectrum $F_{\rm sh}(\omega)$ of the desired shaped pulse, and, accordingly, the needed complex transfer function $H(\omega)$

$$H(\omega) = F_{\rm sh}(\omega)/F_{\rm in}(\omega). \tag{1}$$

It is important to note that the transfer function $G(\omega)$ of the FBG pulse shaper can generally differ from $H(\omega)$. However, they must be equal for the discrete frequencies of the pulse harmonics, i.e.,

$$G(\omega_m) = H(\omega_m) \tag{2}$$

where $\omega_m = m \cdot \omega_0$ is the frequency of the mth pulse harmonic $m = 1, 2, \ldots, N$, where N is the number of the nonzero harmonics in the input-pulse spectrum, and $\omega_0 = 2\pi/T$ is the fundamental frequency. For the sake of simplicity, we assume that the reflection of each uniform grating does not depend of the wavelength. Such an assumption can be made if the grating spectrum is much wider than the spectrum of the input pulse. Thus, the transfer function of M uniform low-reflecting FBGs can be written in the form

$$G(\omega) = \sum_{k=1}^{M} r_k \exp(ik\omega T/M) \tag{3}$$

where $r_k = |r_k| \exp(i\varphi_k)$, and $|r_k|$ and φ_k are the field reflectivity and the reflection phase of the kth grating, respectively. By substituting (3) into (2), we obtain

$$\sum_{k=1}^{M} r_k \exp(ik\omega_m T/M) = H(\omega_m). \tag{4}$$

It is clear that (4) can be considered as a system of N linear equations for N unknown values of the complex reflectivities r_k. Solving this system gives us the required values of the intensity reflectivity $R_k = |r_k|^2$ and the reflection phase φ_k of each grating. Note that according to (3), $G(\omega)$ represents a linear combination of r_k. Therefore, the reflectivity of one of the gratings, for instance the first one, can be taken as given. In this case, the number of gratings should be

$$M = N + 1. \tag{5}$$

It obviously follows from (5) that this type of pulse shaping is extremely suitable for pulse trains with a low number (N) of pulse harmonics (i.e., high duty cycle of the pulse train).

The pulses presented in Fig. 1 are the result of the numerical simulations made according to this approach. The needed transfer function of the shaper was taken in the form $H(m) = 1/(2m+1)$ [12], where m is the number of the pulse harmonics. The input-pulse amplitude was assumed to be $E(t) = \mathrm{sech}[1.76 \cdot t/\tau]$ with the pulse intensity full-width at half-maximum (FWHM) of $\tau = 20$ ps. The pulse period was 125 ps.

III. Simulation Results

For the demonstration of the pulse shaping with uniform FBGs, we chose, as an example, conversion of sinusoidally phase modulated CW light into a Gaussian periodic pulse train. We first performed appropriate simulations. In the simulations, monochromatic CW light is sinusoidally phase modulated, such that $\varphi(t) = A \cdot \cos(\omega_0 t)$, $(\omega_0 = 2\pi f_0)$ with a modulation frequency $f_0 = 10$ GHz and a modulation index $A = 0.8$ rad. Such a periodic optical signal has a field spectrum $F_{\rm in}(\omega_m)$

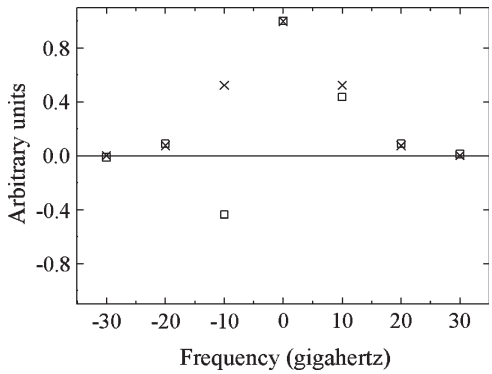

Fig. 2. Calculated field spectra of sinusoidally phase modulated CW light (squares) and of Gaussian periodic pulses (crosses). The modulation frequency is 10 GHz; the modulation index is 0.8 rad; and the intensity width (FWHM) of the Gaussian pulses is 30 ps.

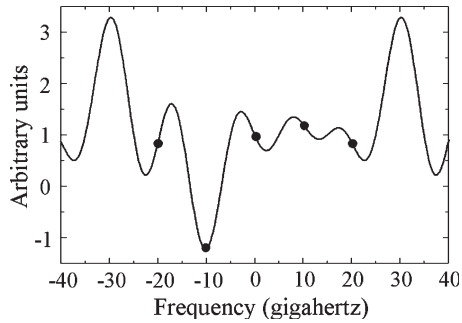

Fig. 3. Calculated transfer function needed for the conversion of the spectra shown in Fig. 2 (circles) and calculated one of the shaper consisting of six FBGs with the parameters given in Table I (solid line).

shown in Fig. 2 (by squares). The phase modulated optical signal is converted to Gaussian periodic pulses with a field amplitude $E_{\rm sh}(t) \propto \exp(-1.386t^2/\tau_G^2)$ having a pulse intensity FWHM of $\tau_G = 30$ ps. The field spectrum $F_{\rm sh}(\omega)$ of the Gaussian pulses is shown in Fig. 2 (by circles). It can be seen from Fig. 2 that the absolute values of the spectra of the input and shaped pulses are very close. Only the harmonics with $m = -1$ have a negative sign. This means that the main action of the pulse shaping in this case is to invert the sign of this harmonic of the input optical signal.

We can see in Fig. 2 that there are only five harmonics in the spectra $F_{\rm in}(\omega_m)$ and $F_{\rm sh}(\omega_m)$, which significantly differ from zero. Therefore, we chose $N = 5$ and the number of the gratings in the shaper $M = N + 1 = 6$. The transfer function $H(\omega_m)$ needed for the reshaping was calculated according to (1), and its values are shown in Fig. 3 (by circles). The system of (4) was solved, and the obtained values of the intensity reflectivity R_k and the reflection phase φ_k of the gratings are presented in Table I. The transfer function of the shaper consisting of the six FBGs calculated according to (3) is shown in Fig. 3 (by solid curve). It can be seen that the values of this transfer functions $G(\omega_m)$ for the frequencies of the harmonics are exactly equal to the needed transfer function $H(\omega_m)$ shown by circles.

The intensity of the shaped pulses is given by a Fourier series

$$I_{\rm sh}(t) \propto \left| \sum_{m=-3}^{3} F_{\rm in}(\omega_m) G(\omega_m) \exp(im\omega_m t) \right|^2. \quad (6)$$

TABLE I
REFLECTIVITY AND REFLECTION PHASE OF EACH FBG CALCULATED AS A SOLUTION OF (4)

Grating #, k	1	2	3	4	5	6
R_k, %	2	0.79	0.89	0.017	0.89	0.79
$\varphi_k/(2\pi)$	0	-0.41	-0.087	0.5	0.087	0.41

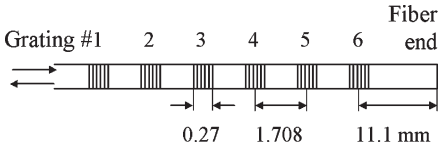

Fig. 4. Pulse shaper consisting of six uniform FBGs.

Fig. 12 (dotted line) shows the shaped Gaussian pulses calculated according to (6).

IV. CONTROL OF THE FBGS DURING THE WRITING PROCESS

It was very important to produce the FBGs with the reflectivities and reflection phases close to the calculated ones (Table I). For the grating control, we followed a method similar to that described on our paper [13]. The method includes the measurement of the reflectivity and reflection phase of each grating and corrections during the writing process until the desired values are obtained. However, in this method, we could not correct the changes in the gratings, which occurred after the grating writing is completed, and therefore, we made modifications.

According to the simulations, we produced an FBG pulse shaper consisting of six FBGs. The Bragg gratings were formed in a boron-doped photosensitive fiber by CW UV radiation ($\lambda = 244$ nm) using a phase mask. The length of each grating was 0.27 mm, enabling an almost constant reflectivity in the region of the pulse spectrum. The spacing between adjacent gratings was 1.708 mm. The gratings were written sequentially, beginning from grating #1 (see Fig. 4).

The FBG control was performed in the following manner. During the grating writing, we probed it with light of spontaneous emission of an erbium-doped fiber amplifier that is reflected from the FBGs and the fiber end (Fig. 4). The reflection was analyzed by an optical spectrum analyzer with a resolution of 0.01 nm. We could neglect the multiple reflections because the reflectivities of the FBGs and the fiber end are low. Thus, we can write the field spectrum $G_{\rm end}(\omega)$ of the gratings together with the fiber end as a sum of the spectra of each element taking into account the phase shifts caused by their different distances from the output plane. The spectrum of the gratings with the fiber end measured by a spectrum analyzer is proportional to $|G_{\rm end}(\omega)|^2$. Thus, we obtain

$$|G_{\rm end}(\omega)|^2 = \left| r_{\rm end} \exp(-2i\omega n l_{\rm end}/c) + \sum_{k=1}^{M} |r_k(\omega)| \exp\left[i\varphi_k(\omega)\right] \exp(-2i\omega n l_k/c) \right|^2 \quad (7)$$

where $r_{\rm end}$ is the field reflectivity of the fiber end, n is the core effective refractive index ($n = 1.462$), c is the velocity of light,

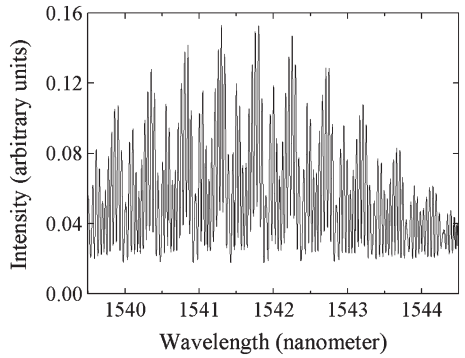

Fig. 5. Spectrum of the reflection from the four written and corrected FBGs and the fiber end.

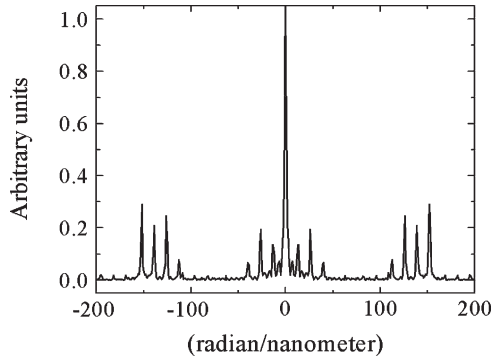

Fig. 6. Absolute value of the Fourier transform of the spectrum shown in Fig. 5. The set of four sidebands on the left and right sides corresponds to the spectral interference between each grating and the fiber end.

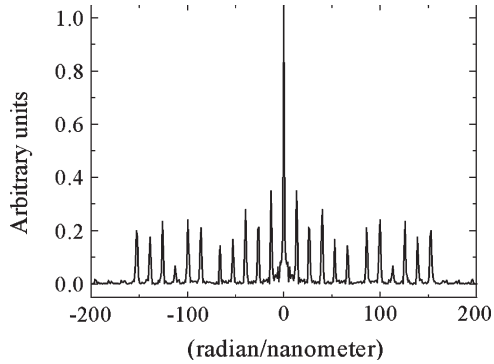

Fig. 7. Absolute value of the Fourier transform for the spectrum of the reflection from the six written and corrected FBGs and the fiber end.

$l_{\rm end}$ and l_k are the distances between the fiber end and kth grating, respectively, and the output plane. It can be seen from (7) that the measured spectrum contains three kinds of the terms:

$$R_{\rm end} + \sum_{k=1}^{M} R_k(\omega) \tag{8}$$

$$|r_k(\omega) r_s(\omega)| \exp\left[i\varphi_k(\omega) - i\varphi_s(\omega)\right] \times \exp\left[-2i\omega(k-s)nL/c\right] \tag{9}$$

$$r_{\rm end}\,|r_p(\omega)| \exp\left[i\varphi_p(\omega)\right] \exp(-2i\omega n L_{pe}/c) \tag{10}$$

where $R_{\rm end}$ and R_k are the intensity reflectivities of the fiber end and kth grating, respectively, s, $p = 1, 2, \ldots, M$, L and $L_{\rm pe}$ are the distances between the adjacent gratings, and between the pth grating and the fiber end, respectively. Term (8) corresponds to the sum of the spectra of all gratings written until that time. Terms (9) and (10) correspond to the interference between the reflections from the kth and sth gratings and from the pth grating and the fiber end, respectively. Term (9) has a factor $\exp[-2i\omega(k-s)nL/c]$ oscillating with ω and a slowly varying amplitude $|r_k(\omega)r_s(\omega)|\exp[i\varphi_k(\omega) - i\varphi_s(\omega)]$. This means that in the Fourier transform of (9), we have a number of bands with finite widths. Analogous bands are obtained by a Fourier transformation of (10). The Fourier transform of (8) gives a contribution to the zero frequency band. If these bands can be separated, we can process the spectral interference pattern (7) as done for the spatial interference case [14].

During the writing process, a fast Fourier transform was performed in real time on the reflection spectrum, measured by an optical spectrum analyzer. For example, we show in Fig. 5 the spectrum measured at the stage when four of the six FBGs were written. The Fourier transform of this spectrum (that also included the reflection from the fiber end) is shown in Fig. 6. The central band in Fig. 6 is the Fourier transform of term (8). By selecting the central band and performing its inverse Fourier transform, we obtain the sum of the spectra of four gratings. For obtaining the spectrum of the currently writing grating (in our example, the fourth written grating #4), we subtracted the known spectra of the previously written gratings. The next three sidebands in Fig. 6 correspond to terms (9). For the measurement of the grating reflection phases $\varphi_p(\omega)$, we used the terms (10), which correspond to the four last sidebands in Fig. 6. For instance, the left sideband in the right set of the four sidebands corresponds to the interference between the grating #4 and the fiber end. By selecting this sideband, taking its inverse Fourier transform and taking argument of the obtained complex values, we obtain, according to (10), the reflection phase $\varphi_4(\omega)$. The distance L_{6e} between the sixth grating and the fiber end was chosen from the condition $L_{6e} > 5L$. In this case, two sets of bands, corresponding to the Fourier transforms of expressions 9 and 10, do not overlap (see Fig. 7).

TABLE II
MEASURED REFLECTIVITY AND REFLECTION PHASE OF EACH FBG

Grating #, k	1	2	3	4	5	6
R_k, %	2	0.784	0.90	0.086	0.90	0.764
$\varphi_k/(2\pi)$	0	-0.42	-0.09	0.49	0.1	0.35

It is important to note that the measurement of the reflectivity and the reflection phase of a currently writing grating were made independently. The grating was written until the needed reflectivity was obtained, and then, the reflection phase was measured. A correction of the reflection phase was performed by UV irradiation without a phase mask of the spacing between the gratings. In such a way, we changed not the phase $\varphi_p(\omega)$ but the refractive index n. It can be seen from (10) that the effect of this action is the same for a fixed frequency.

The measured reflectivities and reflection phases (for $\lambda = 1541.31$ nm) after the corrections for the six FBGs are presented in Table II. It can be seen that the measured values are very close to the calculated ones presented in Table I.

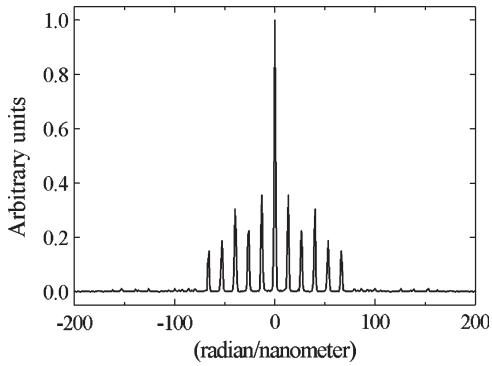

Fig. 8. As those in Fig. 7, when an index-matching gel was deposited on the fiber end of the shaper. It can be seen that the sidebands corresponding to the reflection from the end almost disappear.

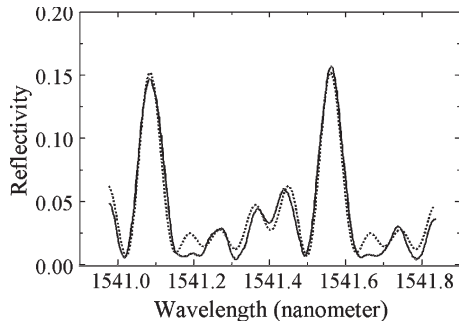

Fig. 9. Reflection spectra of the six FBGs measured (solid curve) and calculated according to (3) with the parameters given in Table I (dotted curve).

In [13], we extracted the information about the phases $\varphi_p(\omega)$ from terms (9). However, it could be made each time only for the last written grating. This means that after completing the writing process, any additional phase correction could not be performed. The use of the fiber-end reflection allows measuring and correction of each grating phase independently and at any time. When we used the FBGs as a shaper, we eliminated the reflection from the fiber end putting on it an index-matching gel. Figs. 7 and 8 show the Fourier transform of the measured spectra of the six corrected FBGs without and with the index-matching gel, respectively. It can be seen in Fig. 8 that the gel removes the fiber-end reflections almost completely. In Fig. 9, we present the measured spectrum of the six corrected FBGs (solid line). For comparison, the spectrum of six FBGs calculated according to (3) is also shown in the figure (dotted line). It can be seen that the two curves are well matched.

V. Experimental Results of Pulse Reshaping

We carried out experiments converting sinusoidal phase modulated CW light into a Gaussian periodic pulse train, which was presented in simulations in Section III. The experimental setup is shown in Fig. 10. The light from a tunable CW laser diode, which was sinusoidally modulated by a LiNbO3 electrooptic phase modulator, was reflected from an FBG shaper and was directed by a circulator to a photodetector and a sampling oscilloscope (50-GHz bandwidth). The phase modulator was driven by an RF signal of 10 GHz formed by a synthesizer and an RF amplifier. An index-matching gel was

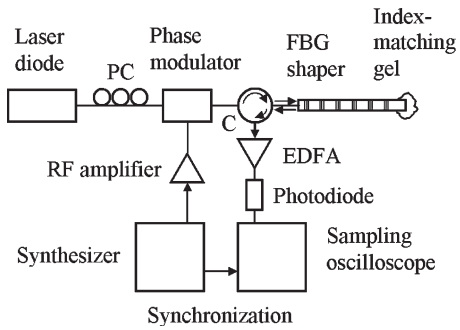

Fig. 10. Experimental setup for the conversion of sinusoidally phase modulated CW light into a Gaussian pulse train: PC—polarization controller and C—circulator.

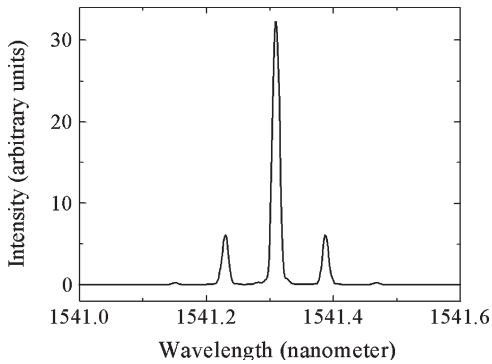

Fig. 11. Laser-diode radiation spectrum taken after sinusoidal-phase modulation.

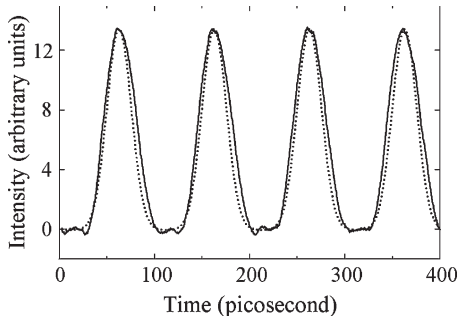

Fig. 12. Shaped Gaussian pulses obtained in the experiment (solid line) and the calculation according to (6) (dotted line).

deposited on the fiber end of the shaper in order to eliminate the reflection from the end. The modulation index was set to 0.8 rad. It was measured from the relation of the components in the spectrum of the light that passed through the phase modulator (see Fig. 11). The energy loss of the input pulses in the pulse shaper was 16 dB. Note that the condition of low grating reflectivity is not a necessary condition in our method of pulse shaping. It only simplifies the calculation and the control of the FBGs. Thus, the grating reflection can be increased such that the energy loss is decreased.

As a result of the pulse reshaping, we obtained nearly Gaussian pulses with a pulsewidth (FWHM) close to 30 ps. An excellent agreement between the calculated and measured shaped pulses can be seen in Fig. 12.

VI. Conclusion

We have demonstrated numerically and experimentally a method for periodic pulse shaping using cascaded uniform FBGs, which is simpler and advantageous over those systems that used complicated structures of FBGs, with or without chirp, and often made by apodization techniques. The principle of the pulse reshaping by uniform FBGs is based on splitting the input optical pulses by weakly reflecting cascaded gratings and superposition of the reflected pulse replicas, each with their own tailored time delay, amplitude, and phase shift determined by the FBGs of the shaper. The superposition of the pulse replicas providing the interference gives the required shape. The needed reflectivity and reflection phase of each grating is unambiguously calculated according to the desirable pulse shape. Because the number of FBGs is determined by the number of pulse train harmonics, this pulse-shaping method is very suitable for the pulse trains with high duty cycle.

We have also developed a method for FBG control during the fabrication process. It includes measurements of the reflectivity and the reflection phase of each grating followed by their corrections. The advantage of the said method is that the measurement of phase deviations and their correction can be made not only during the fabrication process, but at any time after that. Pulse shapers based on uniform FBGs are simple in implementation, potentially low cost, and therefore can find wide applications in various fields, such as in optical communication.

References

[1] A. M. Weiner, "Femtosecond pulse shaping using spatial light modulators," *Rev. Sci. Instrum.*, vol. 71, no. 5, pp. 1929–1960, May 2000.

[2] T. Kurokawa, H. Tsuda, K. Okamoto, K. Naganuma, H. Takenouchi, Y. Inoue, and M. Ishii, "Time–space-conversion optical signal processing using arrayed-waveguide grating," *Electron. Lett.*, vol. 33, no. 22, pp. 1890–1891, Oct. 1997.

[3] A. M. Weiner, J. P. Heritage, and E. M. Kirschner, "High-resolution femtosecond pulse shaping," *J. Opt. Soc. Amer. B, Opt. Phys.*, vol. 5, no. 8, pp. 1563–1572, Aug. 1988.

[4] A. M. Weiner, D. E. Leaird, J. S. Patel, and J. R. Wullert, "Programmable femtosecond pulse shaping by use of a multielement liquid-crystal phase modulator," *Opt. Lett.*, vol. 15, no. 6, pp. 326–328, Mar. 1990.

[5] C. W. Hillegas, J. X. Tull, D. Goswami, D. Strickland, and W. S. Warren, "Femtosecond laser pulse shaping by use of microsecond radio-frequency pulses," *Opt. Lett.*, vol. 19, no. 10, pp. 737–739, May 1994.

[6] D. Meshulach, D. Yelin, and Y. Silberberg, "Adaptive real-time femtosecond pulse shaping," *J. Opt. Soc. Amer. B, Opt. Phys.*, vol. 15, no. 5, pp. 1615–1619, May 1998.

[7] M. Haner and W. S. Warren, "Synthesis of crafted optical pulses by time domain modulation in a fiber-grating compressor," *Appl. Phys. Lett.*, vol. 52, no. 18, pp. 1458–1460, May 1988.

[8] A. Grunnet-Jepsen, A. E. Johnson, E. S. Maniloff, T. W. Mossberg, M. J. Munroe, and J. N. Sweetser, "Fibre Bragg grating based spectral encoder/decoder for lightwave CDMA," *Electron. Lett.*, vol. 35, no. 13, pp. 1096–1097, Jun. 1999.

[9] M. Marano, S. Longhi, P. Laporta, M. Belmonte, and B. Agogliati, "All-optical square-pulse generation and multiplication at 1.5 μm by use of a novel class of fiber Bragg gratings," *Opt. Lett.*, vol. 26, no. 20, pp. 1615–1617, Oct. 2001.

[10] J. Azaña and L. R. Chen, "Synthesis of temporal optical waveforms by fiber Bragg gratings: A new approach based on space-to-frequency-to-time mapping," *J. Opt. Soc. Amer. B, Opt. Phys.*, vol. 19, no. 11, pp. 2758–2769, Nov. 2002.

[11] P. Petropoulos, M. Ibsen, A. D. Ellis, and D. J. Richardson, "Rectangular pulse generation based on pulse reshaping using a superstructured fiber Bragg grating," *J. Lightw. Technol.*, vol. 19, no. 5, pp. 746–752, May 2001.

[12] P. Emplit, M. Haelterman, R. Kashyap, and M. De Lathouwer, "Fiber Bragg grating for optical dark soliton generation," *IEEE Photon. Technol. Lett.*, vol. 9, no. 8, pp. 1122–1124, Aug. 1997.

[13] N. K. Berger, B. Levit, S. Atkins, and B. Fischer, "Repetition-rate multiplication of optical pulses using uniform fiber Bragg gratings," *Opt. Commun.*, vol. 221, no. 4–6, pp. 331–335, Jun. 2003.

[14] M. Takeda, H. Ina, and S. Kobayashi, "Fourier-transform method of fringe-pattern analysis for computer-based topography and interferometry," *J. Opt. Soc. Amer.*, vol. 72, no. 1, pp. 156–160, Jan. 1982.

Naum K. Berger received the M.S. degree in physics from the Novosibirsk State University, Novosibirsk, Russia, in 1967 and the Ph.D. degree in physical electronics (including quantum electronics) from the Institute of Automatics and Electrometry, Novosibirsk, in 1978.

During 1970–1993, he was a Senior Lecturer, Professor at the Physics Department, and Head of the Department of Electrical Engineering at the Khabarovsk State Technical University, Khabarovsk, Russia. Since 1995, he has been a Research Associate at the Technion—Israel Institute of Technology, Haifa, Israel. His research interest is on fiber optics, optical-pulse processing and characterization, and fiber Bragg gratings (FBGs).

Boris Levit received the M.S. degree in physics from the Ural State Technological University, Ekaterinburg, Russia, in 1972 and the Ph.D. degree in radiophysics (including quantum radiophysics) from Moscow State Pedagogical University, Moscow, Russia, in 1982.

Since 1997, he has been a Research Associate at the Electro-Optics Laboratory, Technion—Israel Institute of Technology, Department of Electrical Engineering, Haifa, Israel. His research interests include experimental study of semiconductor and fiber lasers, FBGs, and characterization of ultrashort optical pulses. He has over 40 publications and patents.

Baruch Fischer received the Ph.D. degree from Bar-Ilan University, Ramat Gan, Israel, in 1980.

He was a Weizmann Postdoctorate Fellow at the California Institute of Technology, Pasadena, in 1981–1983. He then joined the Electrical Engineering Department, Technion—Israel Institute of Technology, Haifa, Israel, where he is the Max Knoll Professor in electrooptics and electronics. He served as the Head of the Technion Micro-Electronics Research Center from 1993 to 2001 and as a Dean during 1999–2004. He was a Topical Editor for *Optics Letters* during 1996–2002 and has been on the Editorial Board of the *International Journal of Nonlinear Optical Physics & Materials* since 1992. He has also been a Director of the board of MRV-Communications Inc., Chatsworth, CA, since 1999. His research interest is in nonlinear optics, fiber optics, pulse optics, and statistical mechanics, and quantum mechanics-based study in optics and lasers. In the early 1980s, he was among the founders of the research field of nonlinear photorefractive optics, contributing to the basic wave mixing formalism, the inventions of the first self-pumped phase conjugators, the double phase conjugation, and the first steps in the study of photorefractive self-defocusing and self-trapping and photorefractive solitons. Later, he contributed to the study of nonlinear effects in bacterio rhodopsin and fiber optics. More recently, much of his and his group's research effort is aimed at fiber optics, pulse optics, and short-pulse physics. The latter subject includes a new statistical-mechanics approach to understand the many interacting lightwave modes in lasers that are mostly relevant to pulse formation in mode-locked lasers. This study shows, for example, a thermodynamiclike "melting–freezing" pathway and critical behavior of pulses in mode-locked lasers (similar to gas–liquid–solid and ferromagnetic-phase transitions), explaining, predicting, and observing many exciting features of pulse lasers.

Dr. Fischer is a Fellow of the Optical Society of America.